energies

MDPI

Article

Short-Term Solar Power Forecasting via General Regression Neural Network with Grey Wolf Optimization

Chia-Sheng Tu [1], Wen-Chang Tsai [1], Chih-Ming Hong [2,*] and Whei-Min Lin [1]

[1] School of Mechanical and Electrical Engineering, Xiamen University Tan Kah Kee College, Zhangzhou 363105, China
[2] Department of Electronic Communication Engineering, National Kaohsiung University of Science and Technology, Kaohsiung 811213, Taiwan
* Correspondence: hung71721@nkust.edu.tw

Abstract: With the increasing awareness of environmental protection and the support of national policy, as well as the maturing of solar power generation technology, solar power generation has become one of the most promising renewable energies. However, due to changes in external factors such as season, time, weather, cloud cover, etc., solar radiation is uncertain, and it is difficult to predict energy output, even for the next hour. This inherent instability is a particularly difficult issue for the prediction of energy output in the effective operation of solar power systems. This paper proposes a grey wolf optimization (GWO)-based general regression neural network (GRNN), which is expected to provide more accurate predictions with shorter computational times. Therefore, a self-organizing map (SOM) is utilized to realize the weather clustering and the training of the GRNN with a GWO model. The performance of the proposed model is investigated using short-term and ultra-short-term forecasting in different seasons. It is very important to accurately predict the PV power output. Moreover, the numerical results demonstrate that the proposed approach can significantly enhance the prediction accuracy of PV systems.

Keywords: solar power forecasting; general regression neural network; grey wolf optimization; power generation system

check for updates

Citation: Tu, C.-S.; Tsai, W.-C.; Hong, C.-M.; Lin, W.-M. Short-Term Solar Power Forecasting via General Regression Neural Network with Grey Wolf Optimization. *Energies* **2022**, *15*, 6624. https://doi.org/10.3390/en15186624

Academic Editor: Juan Luis Bosch Saldaña

Received: 22 July 2022
Accepted: 2 September 2022
Published: 10 September 2022

Publisher's Note: MDPI stays neutral with regard to jurisdictional claims in published maps and institutional affiliations.

Copyright: © 2022 by the authors. Licensee MDPI, Basel, Switzerland. This article is an open access article distributed under the terms and conditions of the Creative Commons Attribution (CC BY) license (https://creativecommons.org/licenses/by/4.0/).

1. Introduction

In recent years, due to the rising awareness of environmental protection in the world, the development of diversified clean energy sources has gradually become a requirement. Wind and solar energy are currently the most popular natural energy sources. Especially in urban areas with poor wind conditions, photovoltaic power generation has gradually become the mainstream of renewable energy due to the inexhaustible, clean and pollution-free characteristics of solar energy. Therefore, high-tech countries across the world have focused on investment in research and development with incentives to promote solar photovoltaic systems. The compound growth rate of the global solar cell market has reached 35.5% in the past decade. It has clearly become an emerging hot industry, as indicated by the many solar roof projects and large-scale photovoltaic modules under active construction in various countries [1]. However, photovoltaic power generation depends upon solar irradiance and weather factors; its power generation is a non-steady random process. Many factors could affect the amount of photovoltaic power generated. In order to understand the changes and the impact of photovoltaic power generation, it is necessary to conduct regional installation simulations of photovoltaic power plants and on-site analysis of photovoltaic power generation data. In order to reduce the uncertainty of photovoltaic power generation and supply the power generation of other units to the power company as a reference for power dispatching, it is necessary to analyze the forecast of photovoltaic power generation.

Solar radiation is affected by various random factors, such as the sun's altitude, atmospheric conditions, sunshine duration, and date. With technological development in the meteorological field, many models and methods of physical significance have been presented in the study of solar radiation, such as the solar radiation model, the half-sine model, and the Collares-Pereira and Rabl model. However, these models do not consider the changes in surface solar radiation caused by complex weather and environmental influences; the difference between the calculated results and the actual values is often very high. In addition, it is still very difficult to provide accurate ground solar radiation and power generation forecasts, although current weather forecasting systems have accumulated a huge database. Therefore, it is necessary to further apply artificial intelligence and statistical theories for the analysis of photovoltaic (PV) forecasting. That is, solar power forecasting has been the focus in this study. The related solar-forecasting literature presents numerous models for forecasting solar power generation, and different mathematical models and hybrid mathematical models have been increasingly shown in photovoltaic power simulation. For example, genetic programming (GP) with time series has been presented to predict the power generation of a system; regression analysis has been discussed for the estimation of solar photovoltaic power generation models; and the Montenegro carrot method has been widely used to establish a mathematical model for solving photovoltaic and wind power generation with uncertain climate factors. Forecasts include short-, medium- and long-term solar photovoltaic power generation and wind power generation. Based on historical data, stepwise regression and the group method of data handling (GMDH) have been employed to construct a prediction model of photovoltaic power generation to predict the power generation of a photovoltaic system. At present, many correlation modeling methods such as moving average (MA), auto-regression moving average (ARMA), and autoregressive integrated moving average (ARIMA) can be derived for simulation and analysis from the time series data related to solar photovoltaic power generation [2]. Time series analysis mainly studies the decomposition and prediction of a time series, using the linear auto-regression model (AR) and sliding level of the time series. Traditional time series methods cannot deal with non-linear photovoltaic power generation in a complex and changeable large environment due to the high uncertainties of the environment and climate. Therefore, this paper is mainly focused on various types of neural network-like prediction technologies, which can greatly improve the accuracy of photovoltaic power generation forecasts. The forecast models of photovoltaic power generation can be roughly divided into physical models, statistical models, artificial intelligence models, and hybrid models. Among them, artificial intelligence models are chiefly based on various types of neural networks, such as backpropagation neural networks (BPNN) [3,4], radial basis function neural networks (RBFN) [5,6], and recurrent neural networks (RNN) [7]. Statistical models include the regression model, transfer function model, autoregressive integrated moving average model (ARIMA) [8], Markov chain model [9], and gray model [10]. The main hybrid models for a light radiation prediction are described in the literature [4,11], and related prediction models include the combination of neural networks with wavelet analysis [12], and fuzzy logic [13]; hybrid models such as statistical models and comprehensive models combine short-term and mid-term forecasts. Typical artificial intelligence prediction models are suggested by using artificial neural networks (ANN) and prediction models that combine neural and fuzzy systems [14,15]. In this paper, a new general regression neural network (GRNN) prediction scheme based on grey wolf optimization (GWO) is proposed to more accurately predict PV power generation.

The main contributions of this paper are as follows:

(1) The PV output power of next hours is verified to improve the prediction performance of PV systems.

(2) A SOM framework combined with the GWO_GRNN algorithm is proposed to obtain a prediction model that could provide short-term predictions of PV power output.

(3) The effectiveness of the proposed method is validated by taking real PV data of Taichung, Taiwan. A real variable and SOM variable are used to perform the GRNN with GWO modeling.

2. Data Processing

The photovoltaic modeling data set for predicting solar photovoltaic power generation is shown in Figure 1. It shows solar irradiance and energy across four seasons of the year. Rainy and cloudy weather affect photovoltaic power generation, so solar irradiance will draw proportionally. This section shows the proposed data preprocessing method.

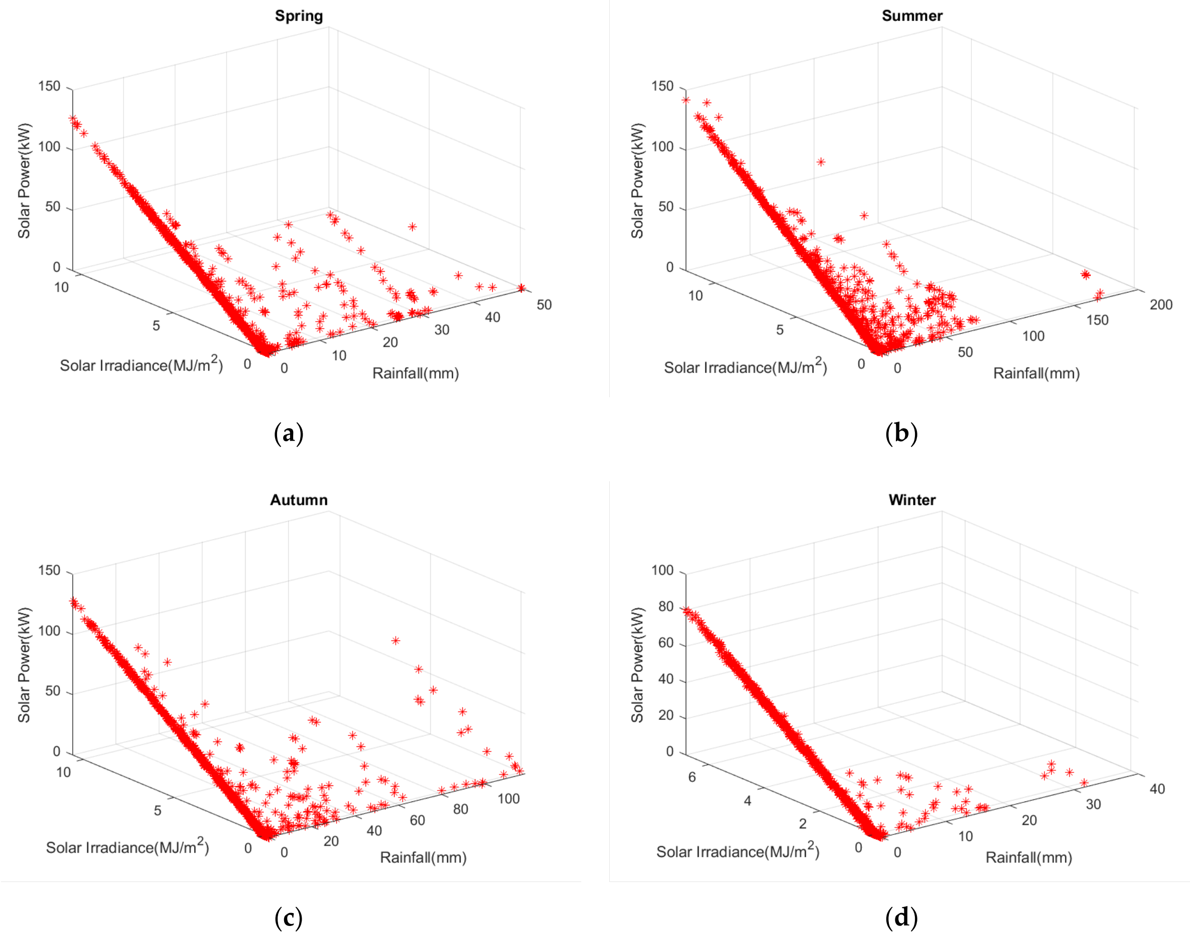

Figure 1. Solar power historical data: (**a**) solar power in spring; (**b**) solar power in summer; (**c**) solar power in autumn; (**d**) solar power in winter.

The data range is from January 2018 to December 2020. There are approximately 52,560 records each year and in total about 157,680 records in the database. Each data item has atmospheric parameters such as wind speed, temperature, relative humidity, and rainfall. The reasons we selected these main variables are: wind speed affects the movement of clouds, temperature reflects the solar insolation, humidity is related to the water vapor in the space, and ultraviolet will be changed to solar irradiance. The other variables ignored generally have little effect.

It is necessary to first determine the year Y and date D to forecast using the database. For example, for a forecast date of 15 April 2020: Y = 2020, and D = 15 April. N1 and N2 represent column and row, in which the row indicates the date (such as 15 April). For example, N1 = 3 indicates the date from D − 3 to D + 3 (a total of seven days from 12 April to 18 April). Column represents the year N2 = 2 indicates the year from 2020 to 2020 − 2 (from 2020 to 2018). Numbers of N1 and N2 can be variable, as seen in Table 1.

Table 1. Iterative strategy for pattern aggregation.

Y, D − 3	Y, D − 2	Y, D − 1	Y, D	Y, D + 1	Y, D + 2	Y, D + 3
Y − 1, D − 3	Y − 1, D − 2	Y − 1, D − 1	Y − 1, D	Y − 1, D + 1	Y − 1, D + 2	Y − 1, D + 3
Y − 2, D − 3	Y − 2, D − 2	Y − 2, D − 1	Y − 2, D	Y − 2, D + 1	Y − 2, D + 2	Y − 2, D + 3

2.1. Weather Clustering

The data group analysis of the second layer is divided into Layers Z21–Z24, as shown in Figure 2. For the topology of Layers Z21–Z24, T and N3 are the time and time interval of input data, respectively. [T − N3] represents six data items in one hour, and T + N3 represents one data item only one hour in the future; that is, one input includes eight data items [T − 6, T − 5, T − 4, T − 3, T − 2, T − 1, T, T + 6].

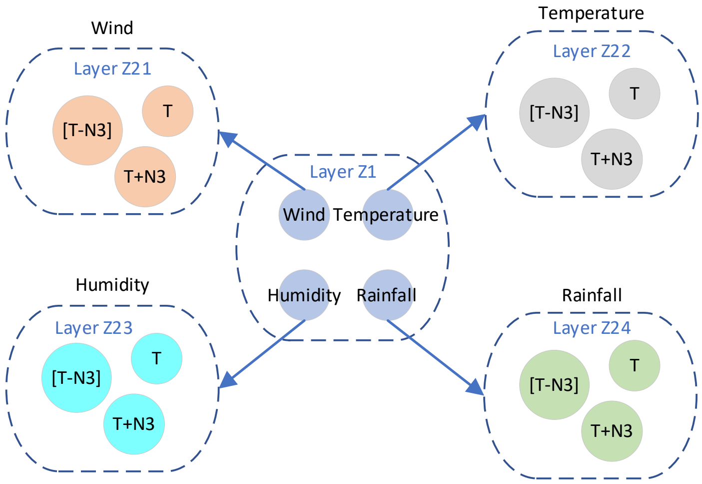

Figure 2. Data group analysis.

Four topological structures (Layer Z21–Layer Z24) are constructed in Layer 2, labeled Z21–Z24, and four classification parameters Z21–Z24 are the integer. Z2 is the expected number of classifications. For example, Z2 = 8 means that the above data could be divided into eight data groups.

2.1.1. Self-Organizing Map Algorithm Flow

Step 1: Initialization.

Link the value vector $w_j(0)$ and set its value in a random manner. All N initial values of the link value vector should be different, and N is the number of class neurons.

Step 2: Input example feature vector.

For time step n, input vector $x = (x_1, x_2, \ldots, x_m)^T$. The input data are wind, temperature, humidity, and rainfall.

Step 3: Find the winner neuron.

By the smallest Euclidean distance, find out the winner neuron j^* at time step n using the following formula:

$$j* = argminjx(n) - wj, j = 1, 2, \ldots, N2$$

Step 4: Adjust the link value vector.

Use the following formula to adjust the link value vector of all neuron types:

$$w_j(n+1) = \begin{cases} w_j(n) + \eta(n)[x(n) - w_j(n)], & j \in N_{j^*}(n) \\ w_j(n), & j \notin N_{j^*}(n) \end{cases}$$

where $\eta(n)$ is the learning rate parameter and $N_{j^*}(n)$ is the neighbor of winner neuron j^*.

Step 5: Go to step two. The algorithm will not be terminated until the feature map is formed. The SOM framework is shown in Figure 3 [16,17].

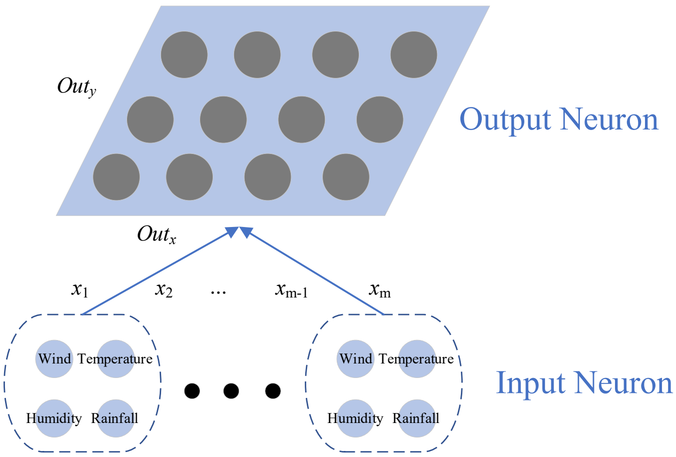

Figure 3. SOM framework.

2.1.2. Photovoltaic Power Generation Model

Solar energy is highly intermittent. Although forecasting is an extremely difficult problem, it is inseparable from the preparations for building solar forecasting models. In this study, the input variables are wind, temperature, humidity, and rainfall, while the output variables are the magnitude of solar power in the next period. A self-organizing map (SOM) is used for one-hour solar power predictions and one-day solar power predictions. Figure 4 shows the building process of the proposed model. Five input styles are included in the prediction model: (i) wind; (ii) temperature; (iii) humidity; (iv) rainfall; and (v) solar irradiance.

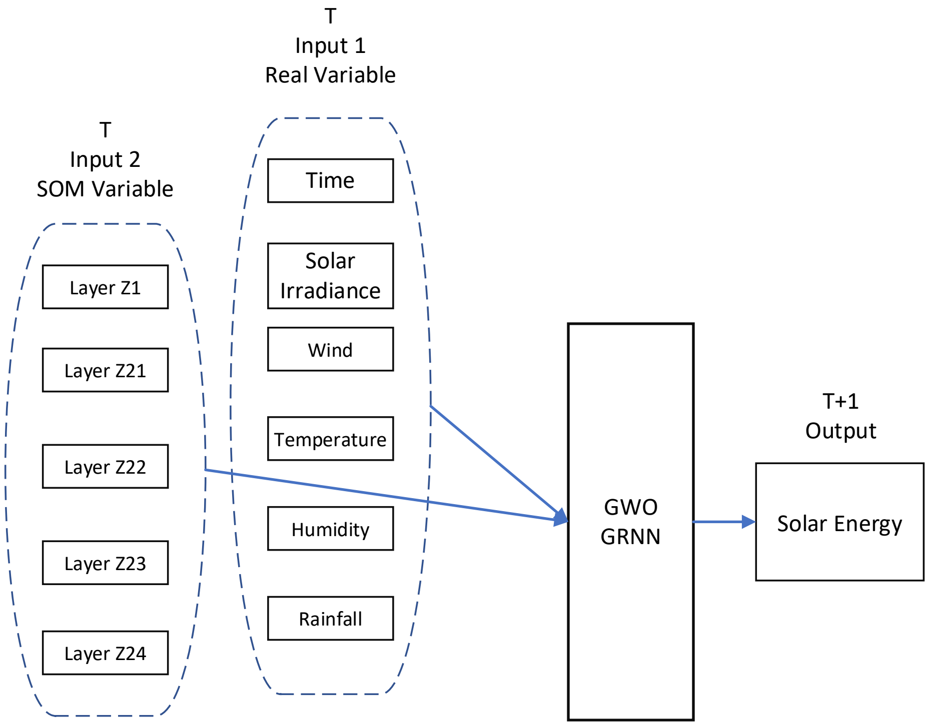

Figure 4. Solar power modeling process.

After the data group analysis of Layer Z1 and Layers Z21–Z24, each piece of data receives a grouping code such as [4, 8, 3, 2, 1] with five integers (1 to 8), representing Input 2 (SOM variable). The predictive model in this paper uses Input 1 + Input 2 to perform the GWO algorithm and GRNN modeling.

(1) Input 1 (real variable) represents the actual value (generally the parameter size, weight, and spacing difference of each datum are different).
(2) Input 2 (SOM variable) represents the value of each data group (which can be clearly classified as the Layer Z1 and Layer Z2) and uses Input 1 + Input 2, as shown in Figure 4.

2.2. Performance Evaluation

The mean relative error (*MRE*), mean absolute error (*MAE*), the mean bias error (*MBE*), root mean squared error (*RMSE*), mean absolute percent error (*MAPE*), normalized mean bias error (*nMBE*), and coefficient of determination (R^2) are widely adopted to assess the performance of solar power forecasting. The evaluation criteria are defined as follows [18,19]:

$$MRE = \frac{1}{N}\sum_{i=1}^{N}\frac{\left|P_i^{real} - P_i^{pred}\right|}{P_{PV}^{capacity}} \times 100\% \tag{1}$$

where N is the number of samples; P_i^{real} is the actual power; and P_i^{pred} is the predicted power.

MAE and *MBE* represent the accuracy in the same data unit, which helps to conceptualize the size of the error. It is expressed by the following equation:

$$MAE = \frac{1}{N}\sum_{i=1}^{N}\left|P_i^{pred} - P_i^{real}\right| \tag{2}$$

$$MBE = \frac{1}{N}\sum_{i=1}^{N}\left(P_i^{pred} - P_i^{real}\right) \tag{3}$$

RMSE is easier to interpret, as it is expressed in the same units as the predictor variable:

$$RMSE = \sqrt{\frac{1}{N}\sum_{i=1}^{N}\left(P_i^{pred} - P_i^{real}\right)^2} \tag{4}$$

MAPE and *nMBE* express the accuracy as a percentage error. Since this number is a percentage, it may be easier to understand than other measurement formulas. It is expressed by the following equation:

$$MAPE = \frac{1}{N}\sum_{i=1}^{N}\frac{\left|P_i^{pred} - P_i^{real}\right|}{P_i^{real}} \times 100\% \tag{5}$$

$$nMBE = \frac{\sum_{i=1}^{N}\left(P_i^{pred} - P_i^{real}\right)}{\sum_{i=1}^{N}P_i^{real}} \times 100\% \tag{6}$$

For the coefficient of determination, the range of R^2 is between 0 and 1. The closer R^2 is to 1, the more efficient and accurate the predictive model is, as well as providing better generalization performance.

$$R^2 = 1 - \frac{\sum_{i=1}^{N}\left(P_i^{real} - P_i^{pred}\right)^2}{\sum_{i=1}^{N}\left(P_i^{real} - P_{avg}\right)^2}, \cdot P_{avg} = \frac{1}{N}\sum_{I=1}^{N} P_i^{real} \tag{7}$$

3. Proposed General Regression Neural Network with Grey Wolf Optimization

3.1. Generalized Regression

GRNN is proposed by Specht as an alternative to the well-known backpropagation training algorithm for feedforward neural networks. This neural network, like other probabilistic neural networks, only needs to backpropagate a small part of the training samples required by the neural network [20–23]. The data obtained from the measurements of an operating system are usually not enough for backpropagation neural networks. Therefore, the use of probabilistic neural networks is particularly advantageous since they can converge to the underlying function of the data, and a few training samples are enough. There is relatively little additional knowledge required to obtain the fit in a satisfactory manner, and it can be completed without additional input from the user.

3.2. Grey Wolf Optimization

In grey wolf optimization (GWO), the optimization solution is alpha (α), beta (β), and delta (δ). The GWO algorithm can be represented by [24–26]

$$X(t+1) = \frac{[X_1(t) + X_2(t) + X_3(t)]}{3} \tag{8}$$

where $X(t+1) = \sigma$ is a smoothness parameter, and $X_1(t)$, $X_2(t)$ and $X_3(t)$ represent position vectors α, β, and δ in the current population, respectively.

$$X_1(t) = |\alpha(t) - R_1(t) \cdot [M_1(t) \cdot \alpha(t) - X(t)]| \tag{9}$$

$$X_2(t) = |\beta(t) - R_2(t) \cdot [M_2(t) \cdot \beta(t) - X(t)]| \tag{10}$$

$$X_3(t) = |\delta(t) - R_3(t) \cdot [M_3(t) \cdot \delta(t) - X(t)]| \tag{11}$$

where $\alpha(t)$, $\beta(t)$, and $\delta(t)$ stand for the three vectors as the three best solutions. $R_1(t)$, $R_2(t)$, $R_3(t)$, and $M_1(t)$, $M_2(t)$, $M_3(t)$ can be calculated as follows:

$$R_1(t) = R_2(t) = R_3(t) = 2c(t)\gamma_1 - d(t) \tag{12}$$

$$M_1(t) = M_2(t) = M_3(t) = 2\gamma_2 \tag{13}$$

where γ_1 and γ_2 are two random vectors in [0,1]. The updated numbers of two adjusted factors, $c(t)$ and $d(t)$, control the tradeoff between exploration and exploitation. Two exponential-functional adjustable factors, $c(t)$ and $d(t)$, express the updated values at iteration according to the following equations:

$$c(t) = 2e^{-t/a_{t1}} \tag{14}$$

$$d(t) = 2e^{-t/a_{t2}} \tag{15}$$

where t indicates the iteration number, and a_{t1} and a_{t2} describe the total number of iterations allowed for the optimization. Finally, $X(t+1) = \sigma$ indicates the best solution in connection with the smoothness parameter of the GRNN. The flowchart of GRNN with the GWO algorithm is shown in Figure 5.

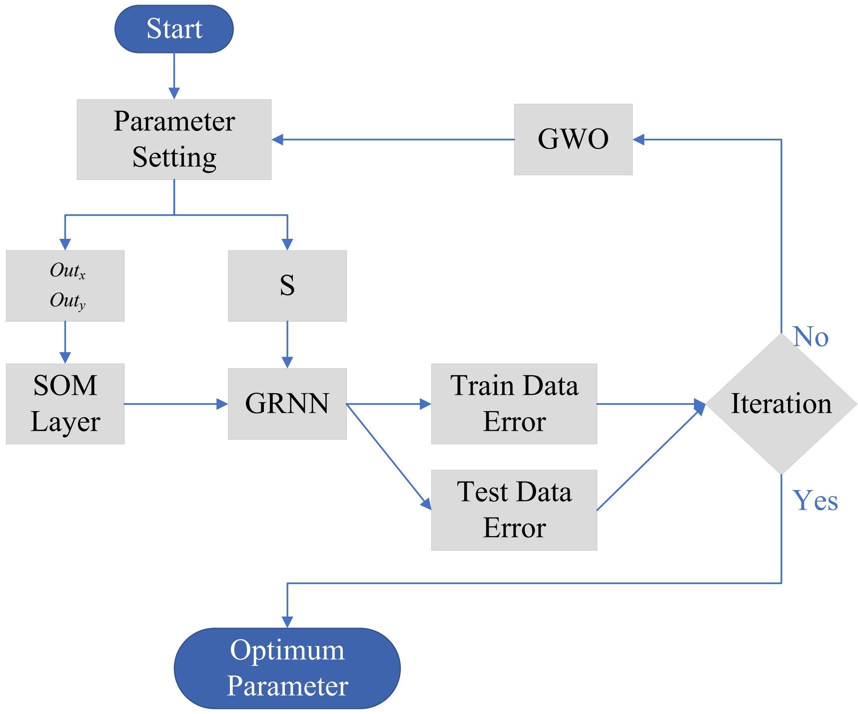

Figure 5. GWO_GRNN flow chart.

4. Numerical Results

The rated power of the PV power plant was 200 kW and the solar power data sets were taken from January 2018 to December 2020 from the Taiwan Power Company's website [27]. The simulation was examined using a computer with an Intel Core i7-3770k 3.5 GHz CPU, 8 GB RAM, and MATLAB R2018a. The data are publicly available for researchers on the Taiwan Central Weather Bureau Automatic Weather Station's website [28].

The GWO_GRNN model is compared with three other models, namely the long short-term memory (LSTM) [29–31], support vector machine (SVM) [32], and GRNN [30], for solar power prediction. Data regression combined with the SOM model was investigated for solar power forecasting.

4.1. Short Term Solar Power Forecasting (Hours)

The one-hour solar power forecasting results are presented in Figure 6. Figure 6b shows the one-hour forecast results for summer. It can be seen from the results that the solar energy had a higher output power, and the summer's prediction was smoother than that in other seasons. The average output power of the proposed algorithm in the four seasons was higher than that of the other strategies, and the solar power in autumn was greater compared with the other seasons, as shown in Figure 6a,b,d. Furthermore, the GWO_GRNN model provided a better performance than the other methods.

4.2. Ultra-Short-Term Solar Forecasting (10 min)

The forecasting results of the proposed method for 10 min solar power are shown in Figure 7. It can be seen from Figure 7 that there was little difference between the GRNN model and the GWO_GRNN model. The forecast was considered from January 2018 to December 2020 during all four seasons. For the ultra-short-term, the proposed GWO_GRNN model had better results than the other models. The proposed model performance in minutes is depicted in Figure 7, having great advantages in improving prediction accuracy. The method effectively combines the advantages of different methods and greatly improves the accuracy of the solar power prediction.

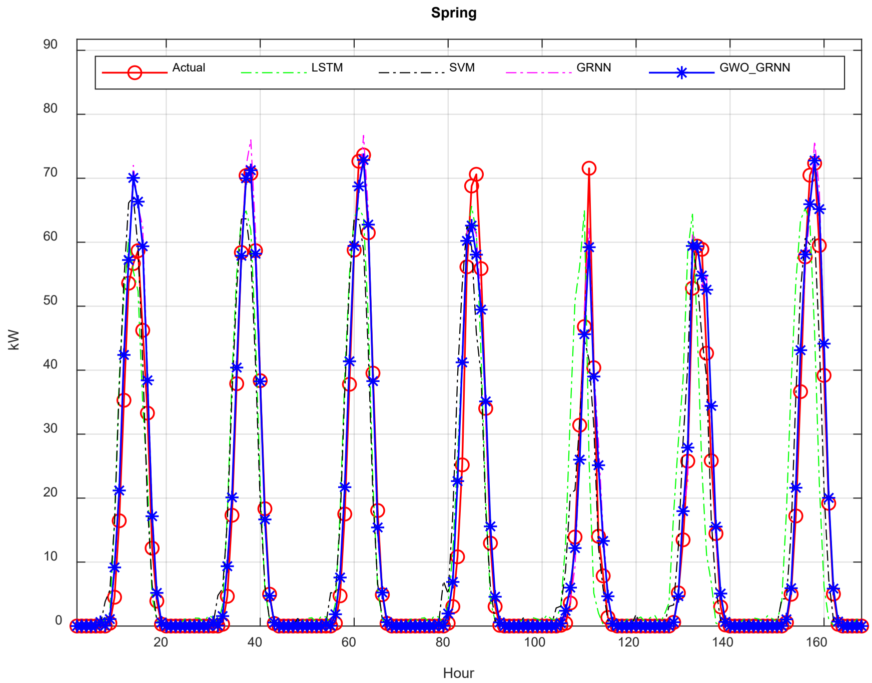

(**a**)

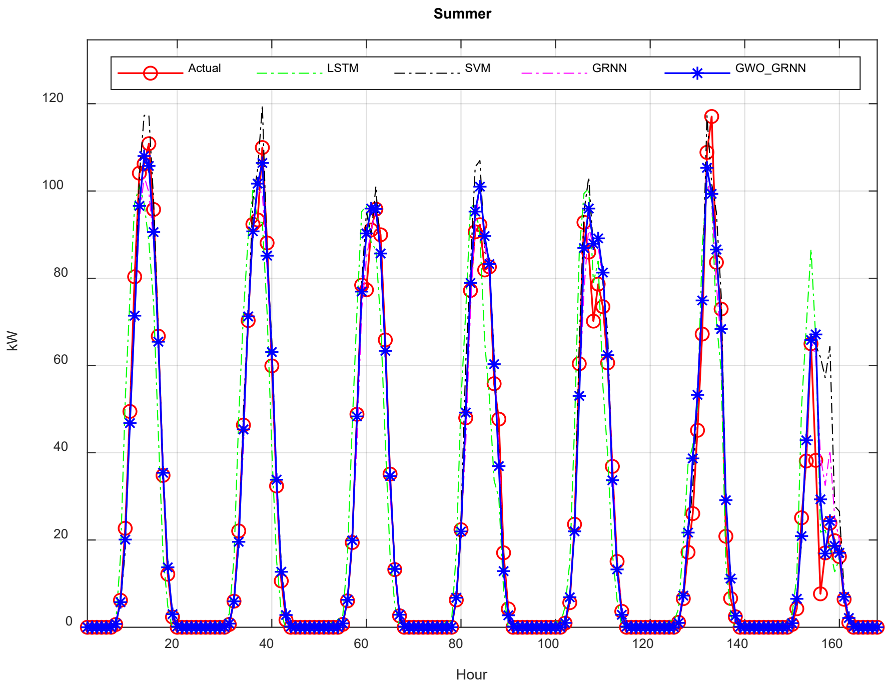

(**b**)

Figure 6. *Cont.*

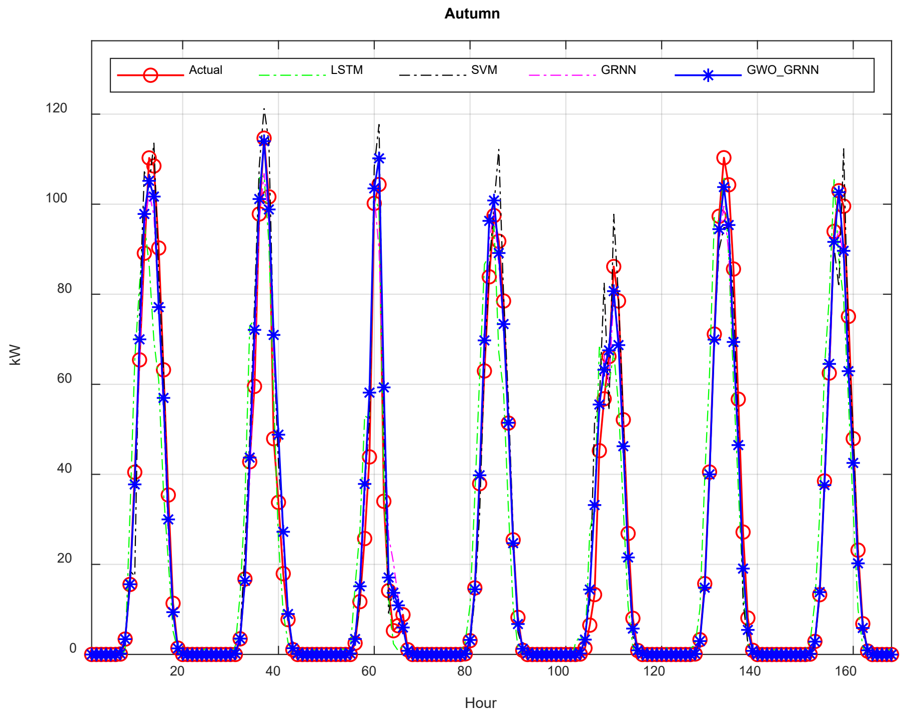

(c)

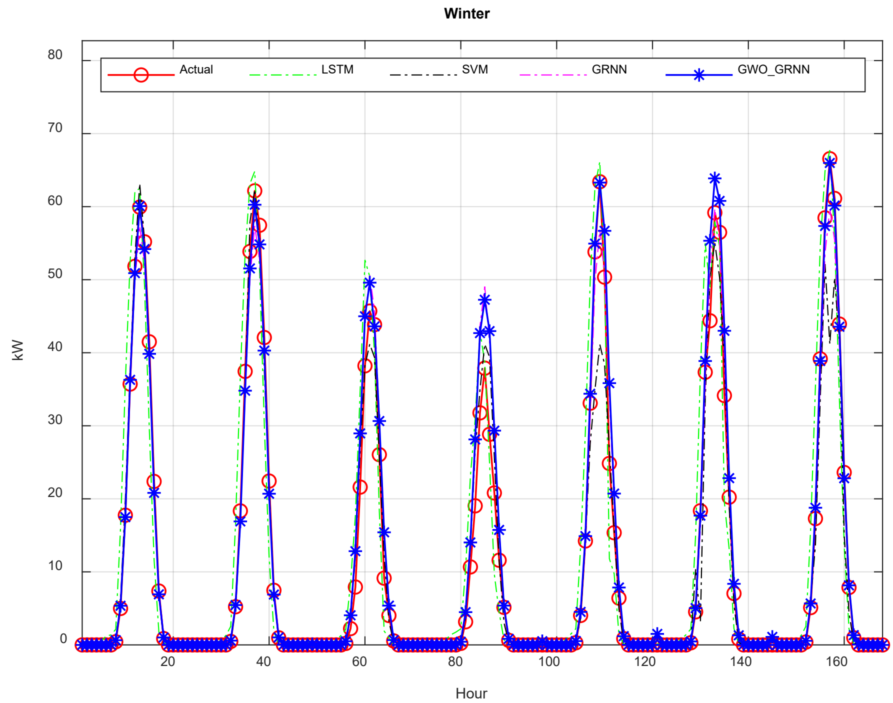

(d)

Figure 6. Seasonal short-term solar power predictions: (**a**) spring, (**b**) summer, (**c**) autumn, and (**d**) winter.

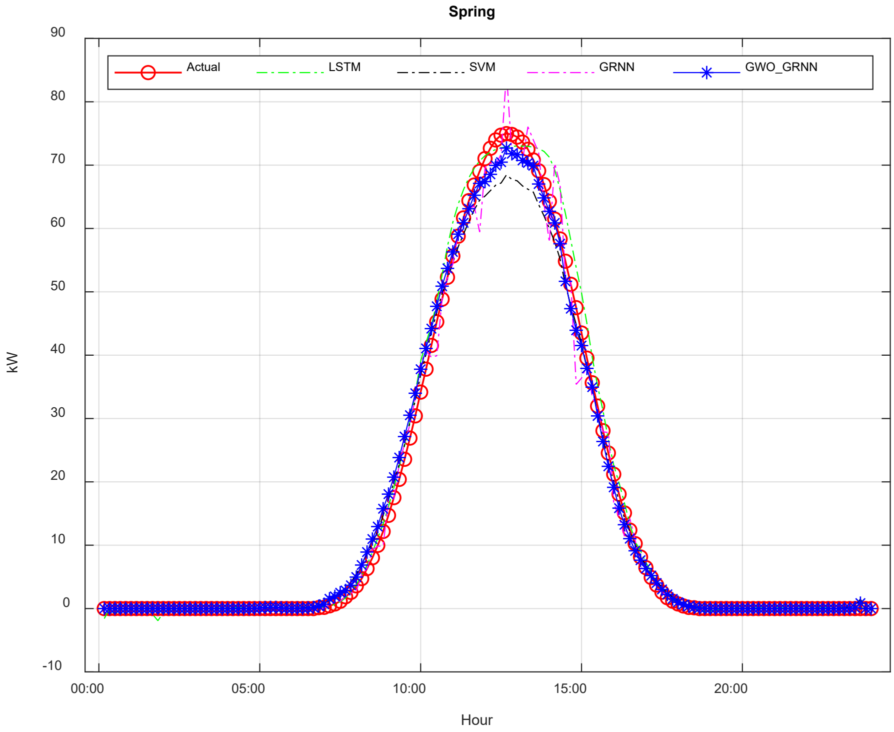

(**a**)

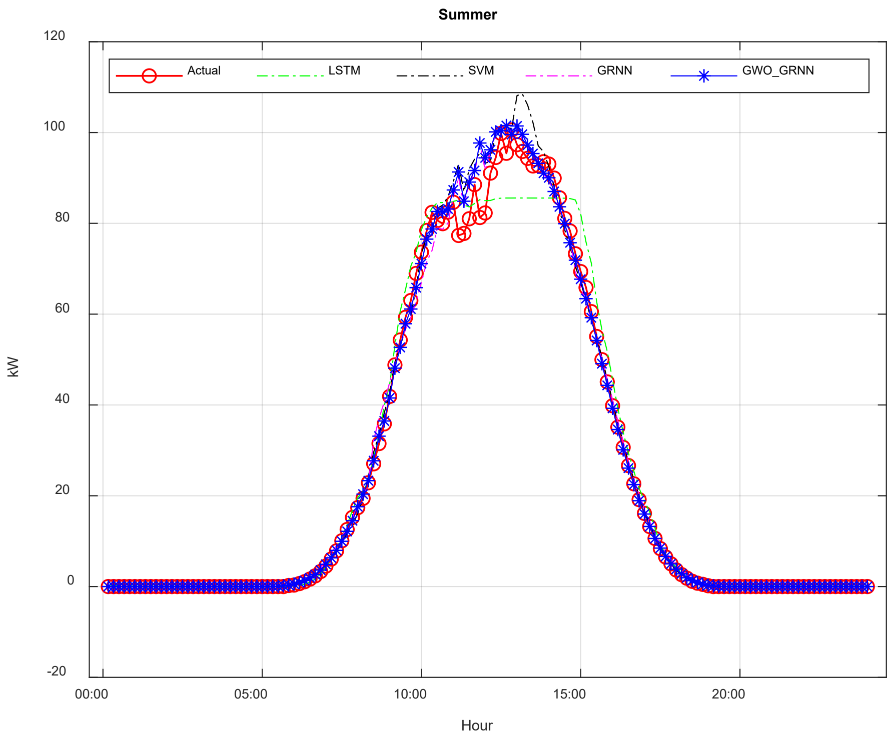

(**b**)

Figure 7. *Cont.*

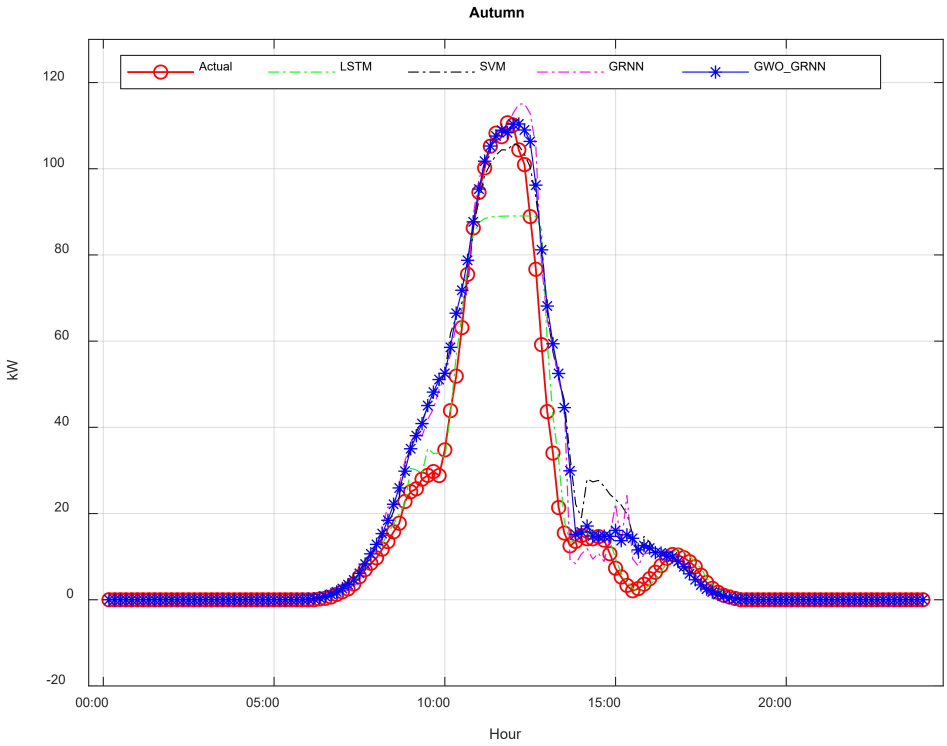

(**c**)

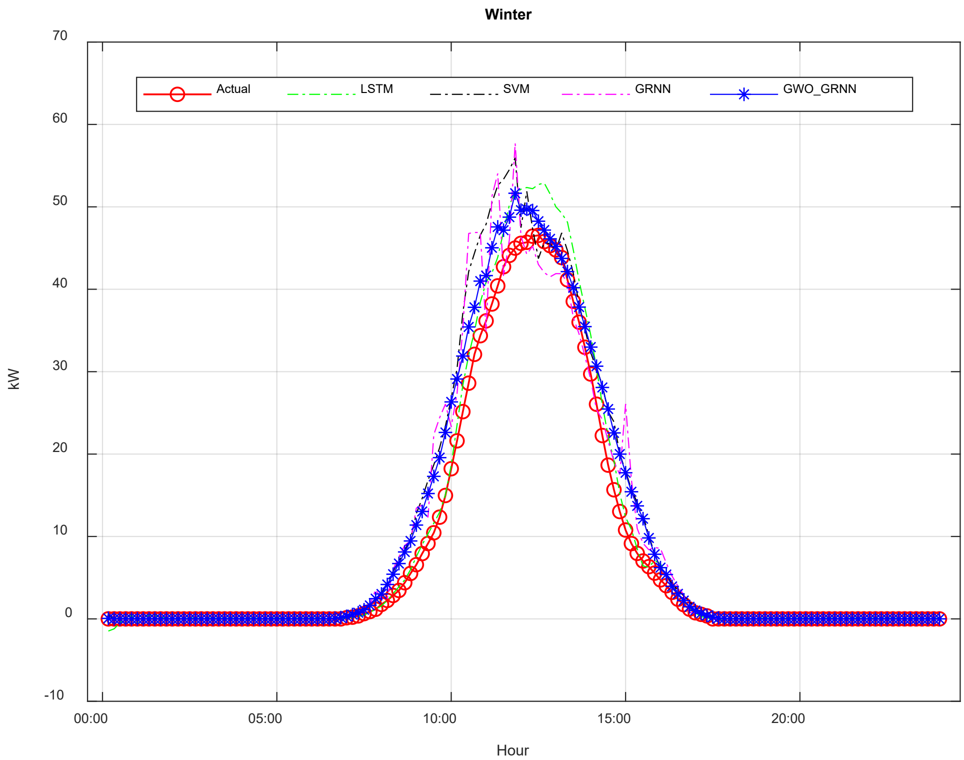

(**d**)

Figure 7. Seasonal ultra-short-term solar power predictions: (**a**) spring, (**b**) summer, (**c**) autumn, and (**d**) winter.

4.3. Stability and Robustness of the Forecasting Model

Numerous simulations were performed on the prediction model to ensure the proposed method could provide stable and reliable prediction results [31]. Figures 8 and 9 present the related error bars of *RMSE* and *MAE* in the spring, summer, autumn, and winter. As the cyclic architecture and storage unit were determined, the *RMSE* and *MAE* of the four seasons were obtained from the proposed method and maintained a low error within the prediction range because the adjacent power data in each prediction process were used. Table 2 shows the *MAE* and *RMSE* of the predicted power output of the all-season forecast.

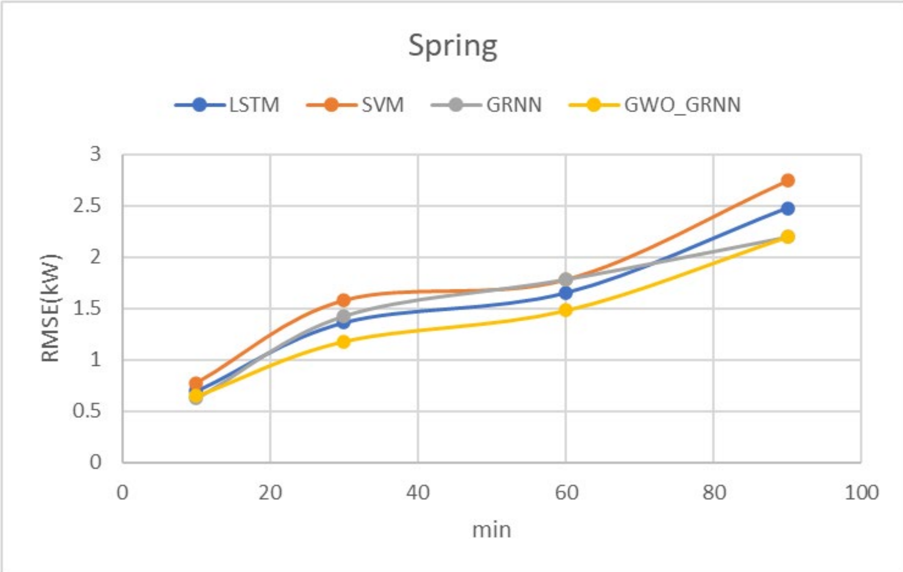

(**a**)

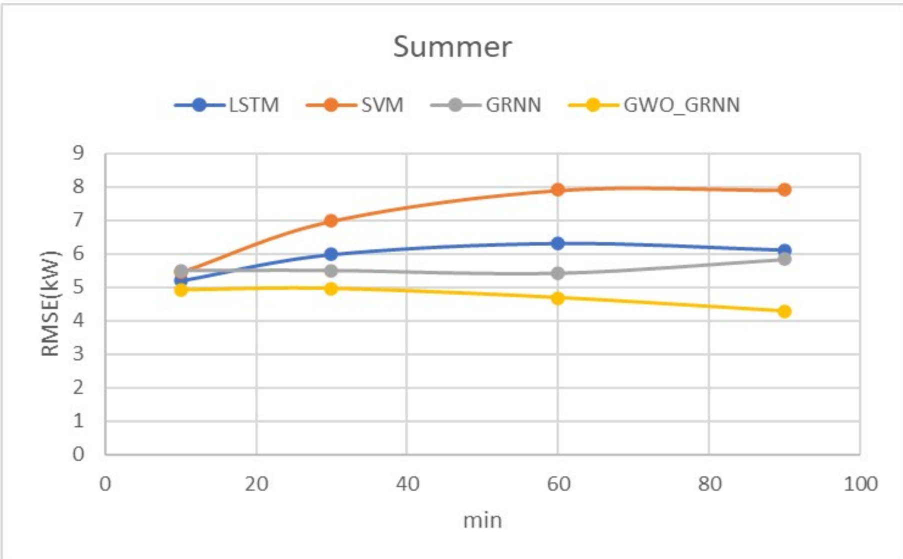

(**b**)

Figure 8. *Cont.*

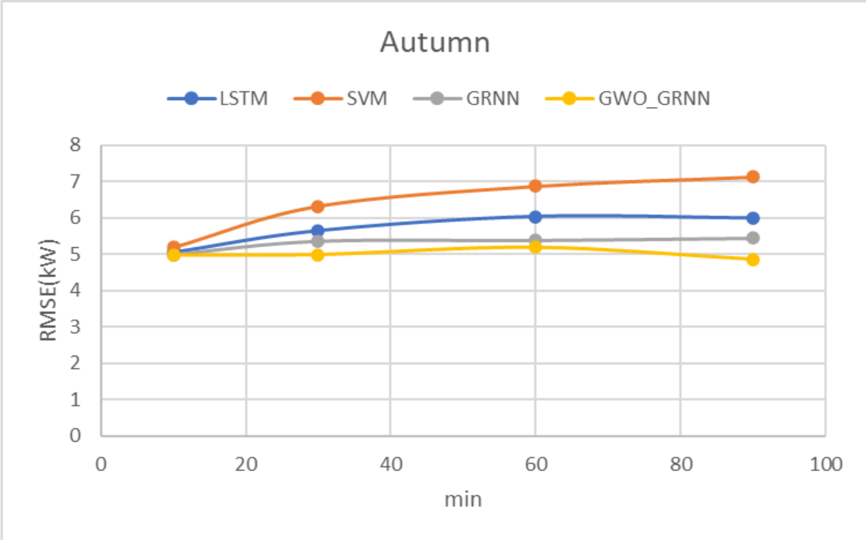

(**c**)

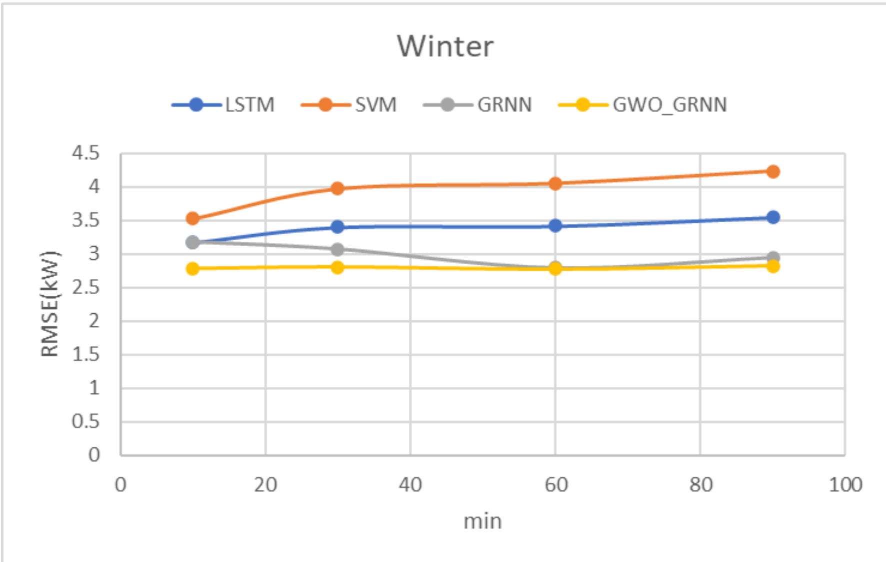

(**d**)

Figure 8. *RMSE* statistics in terms of various forecasting horizons: (**a**) spring, (**b**) summer, (**c**) autumn, and (**d**) winter.

Table 2. Comparison of *MAE* and *RMSE* between the GWO_GRNN and three different methods.

Mean Error	Total Data	min	LSTM	SVM	GRNN	GWO_GRNN
MAE (kW)	4032	10	1.549	1.621	1.555	1.469
	1344	30	1.698	1.927	1.729	1.479
	672	60	1.838	2.138	1.767	1.518
	448	90	1.889	2.274	1.846	1.502
RMSE (kW)	4032	10	3.534	3.736	3.573	3.333
	1344	30	4.100	4.716	3.840	3.484
	672	60	4.356	5.154	3.844	3.533
	448	90	4.534	5.506	4.105	3.539

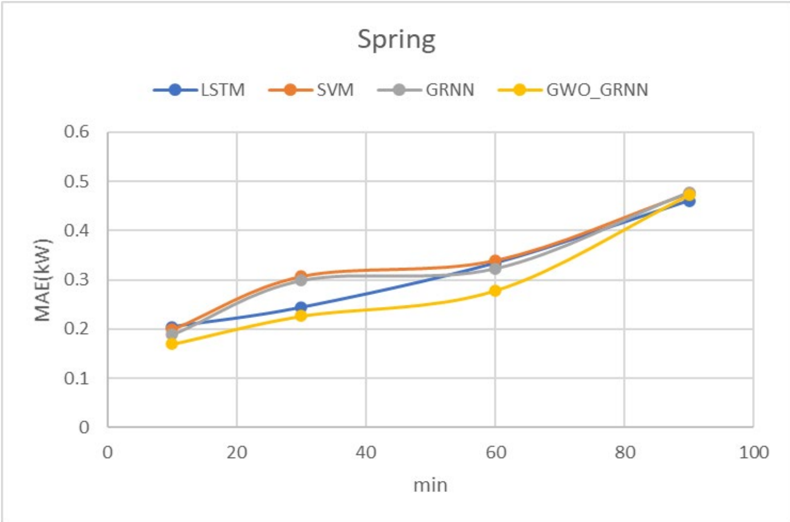

(**a**)

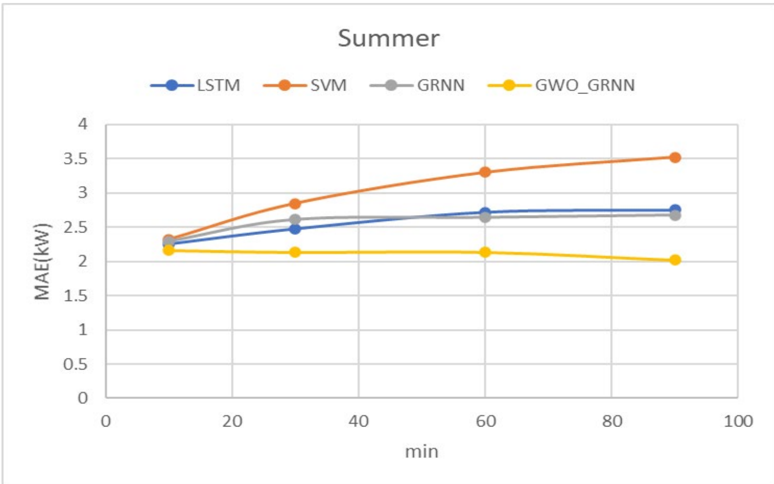

(**b**)

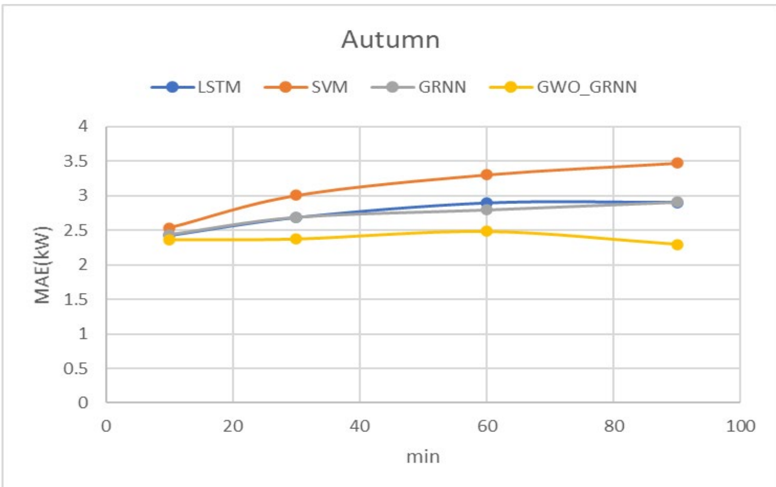

(**c**)

Figure 9. *Cont.*

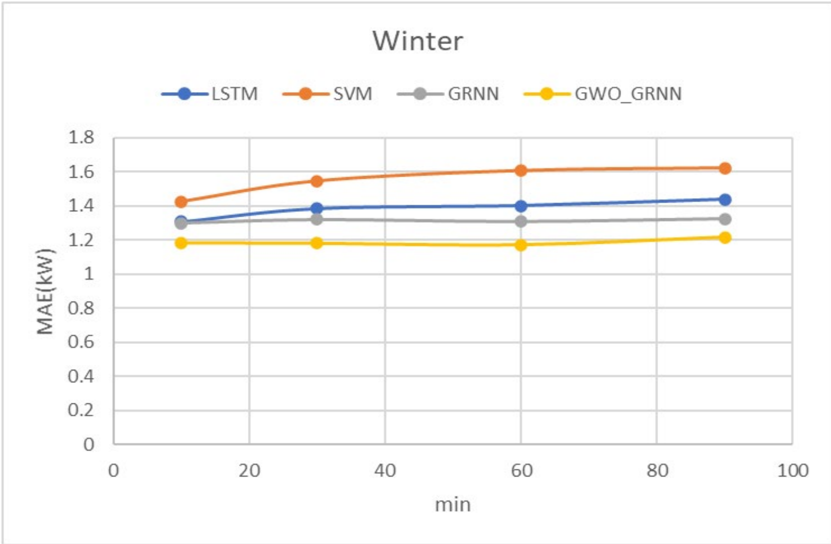

(**d**)

Figure 9. *MAE* statistics in terms of various forecasting horizons: (**a**) spring, (**b**) summer, (**c**) autumn, and (**d**) winter.

The results showed that our method could provide reliable prediction results for photovoltaic power generation. Therefore, from the numerical results, we can easily conclude that the proposed method exhibited the prediction performance of an ideal photovoltaic power generation.

5. Discussion

The performance evaluation of the solar power forecasting used seven evaluation indicators, *MAE*, *RMSE*, *MAPE*, *MRE*, *MBE*, *nMBE*, and R^2, as shown in Table 3. *MAE*, *RMSE*, *MAPE*, *MRE*, *MBE*, *nMBE*, and R^2 have been widely presented to evaluate the performance of solar power forecasting models [19,29–31,33]. The results shown in Figures 6 and 7 and Table 3 were taken from a 24 h period in each season, i.e., 3 December (winter), 3 March (spring), 3 June (summer), and 3 September (autumn). According to the one-hour ahead forecast error, both the forecast errors during each season and the average forecast error were reduced by 0.011%, 0.006%, 0.005%, and 0.027%, respectively. The results in Table 3 show that the prediction accuracy of the GWO_GRNN model was significantly better than that of GRNN, LSTM and SVM. Taking into account the accuracy of GWO_GRNN on average, forecasting accuracy was improved by 13.46%, 17.04% and 28.33% in *MAE* compared to the preceding three methods based on GRNN, LSTM, and SVM, respectively. Similarly, the *RMSE* was improved by 7.28%, 18.1% and 30.71%, respectively. The solar power forecasting errors in all four seasons can be clearly observed. Table 4 shows the average error of the predicted power value of the all-season ultra-short-term forecast. It can be seen that GWO_GRNN improved the search capability and guaranteed the global optimum as far as possible. In Table 4, the GWO_GRNN algorithm showed higher accuracy, while the *MAE*, *RMSE*, *MAPE*, *MRE*, *MBE*, *nMBE*, and R^2 were greater than those in LSTM, SVM, and GRNN.

Table 3. Comparison of performance evaluation for the one-hour-ahead forecasting between the GWO_GRNN and three different methods (Hours).

Seasons	Error	LSTM	SVM	GRNN	GWO_GRNN
Spring (1 March 2020~7 March 2020) Data 168	*MAE* (kW)	2.0299	2.302	1.966	1.743
	RMSE (kW)	4.041	4.557	3.889	3.558
	MAPE (%)	0.0177	0.033	0.023	0.011
	MRE (%)	1.0085	1.151	0.983	0.871
	MBE (kW)	0.5506	0.214	1.120	0.929
	nMBE (%)	0.0083	0.0090	0.0166	0.0079
	R^2	1.0358	1.1148	1.8870	0.9598
Summer (1 June 2020~7 June 2020) Data 168	*MAE* (kW)	2.7282	3.302	2.641	2.133
	RMSE (kW)	6.2856	7.910	5.414	4.687
	MAPE (%)	0.0103	0.040	0.009	0.006
	MRE (%)	1.365	1.651	1.321	1.067
	MBE (kW)	1.5336	2.420	0.473	0.654
	nMBE (%)	0.1052	0.1152	0.2119	0.1004
	R^2	0.3162	1.1776	2.0036	0.9479
Autumn (1 September 2020~7 September 2020) Data 168	*MAE* (kW)	2.9177	3.304	2.795	2.489
	RMSE (kW)	6.0528	6.871	5.384	5.190
	MAPE (%)	0.031	0.018	0.028	0.005
	MRE (%)	1.4345	1.652	1.398	1.245
	MBE (kW)	0.6653	1.028	−0.337	0.346
	nMBE (%)	0.0564	0.0509	0.0982	0.0464
	R^2	1.8784	1.1051	2.1548	0.9600
Winter (1 December 2020~7 December 2020) Data 168	*MAE* (kW)	1.408	1.607	1.309	1.172
	RMSE (kW)	3.4116	4.054	2.794	2.776
	MAPE (%)	0.04	0.050	0.003	0.027
	MRE (%)	0.7189	0.803	0.655	0.586
	MBE (kW)	0.1171	−0.645	0.385	0.863
	nMBE (%)	−0.0958	−0.0656	−0.1292	−0.0586
	R^2	1.1328	1.0164	1.9329	0.9523
Average	*MAE* (kW)	2.2709	2.6287	2.177	1.884
	RMSE (kW)	4.9477	5.848	4.370	4.052
	MAPE (%)	0.0247	0.0352	0.015	0.012
	MRE (%)	1.1317	1.3142	1.089	0.942
	MBE (kW)	0.7166	0.7542	0.410	0.698
	nMBE (%)	0.0185	0.0273	0.049	0.024
	R^2	1.0908	1.1034	1.994	0.955

Table 4. Comparison of ultra-short-term errors for all seasons between the GWO_GRNN and three different methods.

Mean Error	LSTM	SVM	GRNN	GWO_GRNN
MAE (kW)	2.271	2.134	2.041	1.907
RMSE (kW)	4.948	4.652	4.315	4.101
MAPE (%)	0.025	0.002	0.002	0.002
MRE (%)	1.132	1.067	1.021	0.953
MBE (kW)	0.717	0.617	0.518	0.653
nMBE (%)	0.0185	0.0274	0.0494	0.0240
R^2 (%)	1.0908	1.1035	1.9946	0.9550

The simulation results showed that the proposed method based on GWO effectively enhanced the prediction accuracy of short-term solar power generation. In addition, the proposed GWO_GRNN algorithm achieved two goals: improving the accuracy of solar forecasting and reducing its computational cost. Some cases were optimized to illustrate the effectiveness of the algorithm and the results were compared with the results of previous studies. It can be seen from the results that the proposed method was achievable, robust, and more effective than many previously established algorithms.

Furthermore, GRNN had only one parameter having the faster modeling. It has advantages that with GWO it is easier to search for the best parameters to improve the computing performance of the GRNN modeling. It does not mean that the modeling of LSTM and SVM is not as good as that of GRNN, but the size of the solution space is different, so GWO will waste more time and increase the difficulty of finding the best parameters due to other modeling methods requiring more parameters. The more parameters, the larger the solution space and the higher the difficulty. The parameters for the above three methods were adjusted as: (1) GRNN with one parameter, (2) SVM with two parameters, and (3) LSTM more than three parameters.

6. Conclusions

This paper proposed a method to accurately predict short-term photovoltaic power generation due to the intermittent nature of solar power generation. The hybrid method of a data pre-processor based on SOM theory and the GRNN model with GWO was suggested to predict the solar power output within a 24 h time range. The results showed that the prediction accuracy and computational efficiency of this model were better than other models. Predictors and supervised models are useful in many predictions or classification situations, especially when the input data are incomplete or irregular. In order to expand the application of this model, future studies should focus on small-scale power generation, and predict photovoltaic power output using combined global climate, weather and geographic data. The total solar power output could be managed more reasonably and enhance the operational planning and maintenance of photovoltaic power generation. Additionally, the database was used to find clustered data and the SOM was conducted to classify the data cluster in a digital way. This methodology would have better robustness in modeling and effectively avoid large-scale modeling methods. Since the traditional modeling mode has the phenomenon of decimal point or the analogy data interval is too large, the modeling of SOM would classify and convert the analogy data group into a digital data group in the image space so that robustness would be better. Finally, the GRNN model with GWO in comparison with other modeling methods showed better prediction accuracy and computational efficiency in the simulation of photovoltaic power generation.

Author Contributions: C.-S.T. performed the simulations, conducted the concept and application of software. W.-C.T. management activities to annotate (produce metadata), scrub data and maintain research data for initial use and later re-use as well as prepared the revised version. C.-M.H. contributed to the development algorithm and prepared the original draft of the manuscript to be submitted and the revised version. W.-M.L. assisted with analysis of algorithms. All authors have read and agreed to the published version of the manuscript.

Funding: The project was supported by Scholar Research Funds of Xiamen University Tan Kah Kee College (JG2022SRF03 and JG2019SRF05).

Institutional Review Board Statement: Not applicable.

Informed Consent Statement: Not applicable.

Data Availability Statement: Data are contained within the article.

Conflicts of Interest: The authors declare no conflict of interest.

Abbreviations

PV	Photovoltaic
GP	Genetic Programming
GMDH	Group Method of Data Handling
GRNN	General Regression Neural Network
BPNN	Backpropagation Neural Network
RBFN	Radial Basis Function Neural Network
RNN	Recurrent Neural Networks

ANN	Artificial Neural Networks
GWO	Grey Wolf Optimization
GWO_GRNN	General Regression Neural Network with Grey Wolf Optimization
AR	Auto-Regression
MA	Moving Average
ARMA	Auto-Regression Moving Average
ARIMA	Autoregressive Integrated Moving Average
SOM	Self-Organizing Map
MRE	Mean Relative Error
MAE	Mean Absolute Error
MBE	Mean Bias Error
$RMSE$	Root Mean Squared Error
$MAPE$	Mean Absolute Percent Error
$nMBE$	Normalized Mean Bias Error
R^2	Coefficient of Determination
LSTM	Long-Short Term Memory
SVM	Support Vector Machine

Parameters

P_i^{real}	The actual power
P_i^{pred}	The predicted power
P_{avg}	The average power
$X(t+1)$	Smoothness parameter
r_1, r_2	Two random vectors
$c(t), d(t)$	The updated values at iteration
t	The iteration number
a_{t1}, a_{t2}	The total number of iterations

References

1. Solarbuzz. Solar Energymarket Growth: Globalmarket Size. 2010. Available online: www.solarbuzz.com/facts-andfigures/markets-growth/market-growth (accessed on 14 February 2011).
2. Li, Y.; Su, Y.; Shu, L. An ARMAX Model for Forecasting the power output of a grid connected photovoltaic system. *Renew. Energy* **2014**, *66*, 78–89. [CrossRef]
3. Tao, Y.; Chen, Y. Distributed PV power forecasting using genetic algorithm based neural network approach. In Proceedings of the International Conference Advanced Mechatronic Systems, Kumamoto, Japan, 10–14 August 2014; pp. 557–560.
4. Wang, S.; Zhang, N.; Zhao, Y.; Zhan, J. Photovoltaic system power forecasting based on combined grey model and BP neural network. In Proceedings of the International Conference Electrical and Control Engineering (ICECE), Yichang, China, 16–18 September 2011; pp. 4623–4626.
5. Ciabattoni, L.; Ippoliti, G.; Longhi, S.; Cavalletti, M.; Rocchetti, M. Solar irradiation forecasting using RBF networks for PV systems with storage. In Proceedings of the IEEE International Conference Industrial Technology (ICIT), Athens, Greece, 19–21 March 2012; pp. 699–704.
6. Li, Z.Y.; Zhou, Y.L.; Cheng, C.; Li, Y.; Lai, K.X. Short term photovoltaic power generation forecasting using RBF neural network. In Proceedings of the Chinese Control and Decision Conference (CCDC), Changsha, China, 29 May–2 June 2014; pp. 2758–2763.
7. Capizzi, G.; Napoli, C.; Bonanno, F. Innovative second-generation wavelets construction with recurrent neural networks for solar radiation forecasting. *IEEE Trans. Neural Netw. Learn. Syst.* **2012**, *23*, 1805–1815. [CrossRef] [PubMed]
8. Kardakos, E.G.; Alexiadis, M.C.; Vagropoulos, S.I.; Simoglou, C.K.; Biskas, P.N.; Bakirtzis, A.G. Application of time series and artificial neural network models in short-term forecasting of PV power generation. In Proceedings of the International Universities Power Engineering Conference (UPEC), Dublin, Ireland, 2–5 September 2013; pp. 1–6.
9. Li, Y.Z.; Niu, J.C. Forecast of power generation for grid-connected photovoltaic system based on Markov chain. In Proceedings of the Asia-Pacific Power and Energy Engineering Conference (APPEEC), Wuhan, China, 28–30 March 2009; pp. 1–4.
10. Huang, C.Y.; Tzeng, W.C.; Liu, Y.W.; Wang, P.Y. Forecasting the global photovoltaic market by using the GM(1,1) grey forecasting method. In Proceedings of the IEEE Green Technologies Conference, Baton Rouge, LA, USA, 15–6 April 2011; pp. 1–5.
11. Haque, A.U.; Nehrir, M.H.; Mandal, P. Solar PV power generation forecast using a hybrid intelligent approach. In Proceedings of the IEEE Power and Energy Society General Meeting, Vancouver, BC, Canada, 21–25 July 2013; pp. 1–5.

12. Yang, Y.; Dong, L. Short-term PV generation system direct power prediction model on wavelet neural network and weather type clustering. In Proceedings of the International Conference Intelligent Human-Machine Systems and Cybernetics, Hangzhou, China, 26–27 August 2013; pp. 207–211.
13. Mellit, A.; Hadjarab, A.; Khorissi, N.; Salhi, H. An ANFIS-based forecasting for solar radiation data from sunshine duration and ambient temperature. In Proceedings of the IEEE Power Engineering Society General Meeting, Tampa, FL, USA, 24–28 June 2007; pp. 1–6.
14. Yang, H.T.; Huang, C.M.; Huang, Y.C.; Pai, Y.S. A weather-based hybrid method for 1-day ahead hourly forecasting of PV power output. *IEEE Trans. Sustain. Energy* **2014**, *5*, 917–926. [CrossRef]
15. Sansa, I.; Missaoui, S.; Boussada, Z.; Bellaaj, N.M.; Ahmed, E.M.; Orabi, M. PV power forecasting using different artificial neural networks strategies. In Proceedings of the IEEE International Green Energy, Long Beach, CA, USA, 24 November 2014; pp. 54–59.
16. Felix, M.R.; Sina, K.; Stefan, H. Supervised and Semi-Supervised Self-Organizing Maps for Regression and Classification Focusing on Hyperspectral Data. *Remote Sens.* **2020**, *12*, 7.
17. Hsu, S.H.; Hsieh, J.P.A.; Chih, T.C.; Hsu, K.C. A two-stage architecture for stock price forecasting by integrating self-organizing map and support vector regression. *Expert Syst.* **2009**, *36*, 7947–7951. [CrossRef]
18. Alencar, D.B.; Affonso, C.M.; Oliveira, R.C.L.; Rodríguez, J.L.M.; Leite, J.C.; Filho, J.C.R. Different models for forecasting wind power generation: Case study. *Energies* **2017**, *10*, 1976.
19. Chang, X.; Li, W.; Zomaya, A.Y. A Lightweight Short-Term Photovoltaic Prediction for Edge Computing. *IEEE Access* **2020**, *4*, 946–955. [CrossRef]
20. Kenji, N.F.; Anna, D.P.L.; Carlos, R.M. Short-term multinodal load forecasting using a modified general regression neural network. *IEEE Trans. Power Deliv.* **2011**, *26*, 2862–2869.
21. Specht, D.F. Probabilistic neural network for classification, mapping, or associative memory. In Proceedings of the IEEE International Conference Neural Network, San Diego, CA, USA, 24–27 July 1988; pp. 525–532.
22. Hong, C.M.; Cheng, F.S.; Chen, C.H. Optimal Control for Variable-Speed Wind Generation Systems using General Regression Neural Network. *Int. J. Electr. Power Energy Syst.* **2014**, *60*, 14–23. [CrossRef]
23. Parzen, E. On estimation of a probability density function and mode. *Annals. Math. Stat.* **1962**, *33*, 1065–1076. [CrossRef]
24. Zhang, Y.; Liu, D.; Liu, J.; Xian, Y.; Wang, X. Improved Deep Neural Network for OFDM Signal Recognition Using Hybrid Grey Wolf Optimization. *IEEE Access* **2020**, *8*, 133622–133632. [CrossRef]
25. Majhi, D.; Rao, M.; Sahoo, S.; Dash, S.P.; Mohapatra, D.P. Modified Grey Wolf Optimization(GWO) based Accident Deterrence in Internet of Things (IoT) enabled Mining Industry. In Proceedings of the 2020 International Conference on Computer Science, Engineering and Applications (ICCSEA), Gunupur, India, 13–14 March 2020.
26. Han, S. Modified Grey-Wolf Algorithm Optimized Fractional-Order Sliding Mode Control for Unknown Manipulators with a Fractional-Order Disturbance Observer. *IEEE Access* **2020**, *8*, 18337–18349. [CrossRef]
27. Taiwan Power Company. Available online: https://www.taipower.com.tw/tc/page.aspx?cchk=b6134cc6-838c-4bb9-b77a-0b0094afd49d&cid=406&mid=206 (accessed on 1 January 2021).
28. Taiwan Central Weather Bureau Automatic Weather Station. Available online: http://farmer.iyard.org/ (accessed on 1 January 2021).
29. Li, G.; Xie, S.; Wang, B.; Xin, J.; Li, Y.; Du, S. Photovoltaic Power Forecasting with Hybrid Deep Learning Approach. *IEEE Access* **2020**, *8*, 175871–175880. [CrossRef]
30. Hossain, M.S.; Mahmood, H. Short-Term Photovoltaic Power Forecasting Using an LSTM Neural Network and Synthetic Weather Forecast. *IEEE Access* **2020**, *8*, 172524–172533. [CrossRef]
31. Li, G.; Wang, H.; Zhang, S.; Xin, J.; Liu, H. Recurrent Neural Networks Based Photovoltaic Power Forecasting Approach. *Energies* **2019**, *12*, 2538. [CrossRef]
32. Shi, J.; Lee, W.J.; Liu, Y.; Yang, Y.; Wang, P. Forecasting Power Output of Photovoltaic Systems Based on Weather Classification and Support Vector Machines. *IEEE Trans. Ind. Appl.* **2015**, *48*, 1064–1069. [CrossRef]
33. Wang, H.; Yi, H.; Peng, J.; Wang, G.; Liu, Y.; Jiang, H.; Liu, W. Deterministic and probabilistic forecasting of photovoltaic power based on deep convolutional neural network. *Energy Convers. Manag.* **2017**, *153*, 409–422. [CrossRef]